High-performance olefin polymerization catalysts discovered on the basis of a new catalyst design concept

Tomoaki Matsugi and Terunori Fujita*

This *critical review* highlights the "ligand oriented catalyst design concept", a new catalyst design concept for olefin polymerization that has led to the development of high-activity catalysts. The concept has created a series of highly active ethylene polymerization catalysts, many of which show high activities comparable to those of group 4 metallocene catalysts. Moreover, these catalysts display unique polymerization catalysis to produce a wide variety of polymers that possess unprecedented molecular architectures that are either difficult or impossible to achieve using conventional catalysts (98 references).

1   Introduction

Olefin-based polymers, such as polyethylenes (PEs), polypropylenes (PPs), ethylene/α-olefin amorphous copolymers and ethylene/propylene/diene elastomers (EPDMs), are by far the most important and thus the most produced synthetic polymers today. These polymers possess an amazingly broad range of practical applications due to their cost effectiveness and low density, their broad-ranging material properties, and their outstanding resistance to chemical environments. The applications include plastic shopping bags, food packages, squeeze bottles, containers, storage boxes, toys, disposable diapers, bullet-proof vests, gasoline tanks and car bumpers, making these polymers indispensable materials for modern living.

While the multi-sited heterogeneous Ziegler–Natta catalysts represented by $MgCl_2$-supported $TiCl_4$ catalysts currently dominate the market, single-site catalysts represented by group 4 metallocene catalysts and constrained-geometry catalysts (CGCs) are gaining an increasing presence in the market.[1–3] Benefits of these single-site catalysts include the

Mitsui Chemicals, Inc., Research Center, 580-32 Nagaura, Sodegaura-City Chiba 299-0265 Japan

ability to produce polymers with controlled molecular weight, specific tacticity, improved molecular weight distribution, and better comonomer distribution and content. Because of these advantages, in recent years, the above single-site catalysts have enjoyed success in the commercial production of various polymers with enhanced performance qualities, such as linear low-density PEs, isotactic and syndiotactic PPs (iPPs and sPPs), syndiotactic polystyrenes (sPSs) and ethylene/1-butene amorphous copolymers.

Following the ground-breaking advances made by group 4 metallocene catalysts and CGCs in the syntheses of olefin-based polymers with controlled microstructures, attention has been directed toward the development of new catalysts that provide ever-higher catalyst productivity and greater control over polymer microstructures. As a result of a tremendous amount of academic and industrial research, a diverse number of new and highly potent catalysts based on both early and late transition metals have now been discovered, some of which have provided access to distinctive polymers previously unobtainable with conventional catalysts [*e.g.*, hyperbranched PEs, ethylene/methyl acrylate copolymers, α-olefin-based block copolymers].[4–10]

In our own effort to acquire new high-performance catalysts, we have carried out research based on a "ligand oriented

Tomoaki Matsugi graduated in chemistry from Kyushu University where he received his MS degree working with Professor Seiji Shinkai and Itaru Hamachi. He joined Mitsui Petrochemical Industries, Ltd (now Mitsui Chemicals, Inc.) in 1997. His research interests are focused on the development of olefin polymerization catalysts and valuable polyolefin-based materials.

Terunori Fujita is the general manager of the catalysis science laboratory of Mitsui Chemicals, Inc., and a Mitsui research fellow. His research interests have focused on the synthesis of valuable organic materials with high efficiency using homogeneous and heterogeneous catalysis, and is now engaged in the development of high-performance olefin polymerization catalysts and their applications to new value-added olefin-based materials.
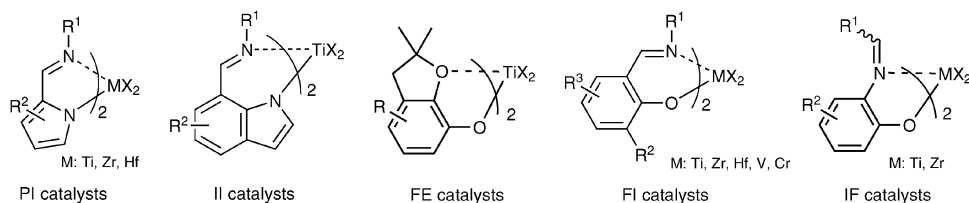
Fig. 1 Examples of highly active catalysts discovered on the basis of the "ligand oriented catalyst design concept".

catalyst design concept", a concept that is founded on the belief that a flexible electronic nature of a ligand is a requirement for achieving high activity. In our studies, we have deliberately focused on non-symmetric ligands since transition metal complexes incorporating such ligands have been investigated less as olefin polymerization catalysts.[11,12]

Such approaches have resulted in the discovery of a number of highly active catalysts, including bis(pyrrolide-imine) group 4 transition metal complexes (PI catalysts), bis(indolide-imine) Ti complexes (II catalysts), bis(phenoxy-ether) Ti complexes (FE catalysts), bis(phenoxy-imine) early transition metal complexes (FI catalysts) and bis(imine-phenoxy) Ti and Zr complexes (IF catalysts) (Fig. 1).[13–18]

Many of these catalysts not only exhibit high ethylene polymerization activities comparable to those obtained with group 4 metallocene catalysts and CGCs, but have also afforded a wide variety of olefin-based polymers with unique architectures. The polymers include selective vinyl- and Al-terminated PEs,[19–21] well-defined and controlled multimodal PEs,[22,23] ultra-high molecular weight ethylene/propylene copolymers,[24] and stereo- and regioirregular high-molecular-weight poly(higher α-olefin)s.[25–27] In addition, these catalysts can produce highly isotactic and syndiotactic PPs[28–33] and polyolefinic block copolymers from ethylene, propylene, higher α-olefins and norbornene.[33–39] Moreover, and importantly, research on these catalysts for olefin polymerization has provided a lot of information on polymerization catalysis and mechanisms, including stereochemical and electronic requirements for accomplishing high activity,[11–15] highly syndioselective propylene polymerization with a C_2-symmetric catalyst,[32] high-incorporation ability for higher α-olefins and norbornene,[13,14,27,39] and thermally robust living olefin polymerization.[33–39] Therefore, we have developed a new series of catalysts according to the ligand oriented catalyst design concept that offer extraordinary opportunities to synthesize olefin-based polymers possessing distinctive architectural characteristics and at the same time a chance to study catalysis and mechanisms for olefin polymerization. Recent work conducted by Bochmann, Busico, Cavallo, Chadwick, Coates, Erker, Gibson, Johnson, Mashima, Mülhaupt, Pellecchia, Repo, Scott, Talarico, Talsi, Ziegler and others have made significant contributions to the further development of the catalysts described herein.[7,13–15,36,40–57]

This review introduces a new catalyst design concept for olefin polymerization and the discovery of new high-activity catalysts that are based on this concept. Additionally, the review describes the unique polymerization catalysis of the new catalysts and the associated syntheses of distinctive polymers, mainly highlighting our own research.

2 Catalyst design concept

Historically, the discovery of highly active catalysts for ethylene polymerization has been the key to creating novel polymers with differentiated macromolecular structures, as is clearly demonstrated by the discovery of TiCl$_4$/R$_3$Al catalysts, MgCl$_2$-supported TiCl$_4$ catalysts, group 4 metallocene catalysts and CGCs.[3] Learning from this history, we decided to pursue high activity since it would be the most fundamental prerequisite for catalysis. We believe that a high-activity catalyst that can bear modification enough to enhance a specific selectivity would in turn result in a desired product with satisfactory efficiency. Accordingly, the purpose of this research has been the discovery of high-activity ethylene polymerization catalysts and their applications to value-added olefin-based polymers with new or improved material properties.

A transition-metal-based olefin polymerization catalyst normally consists of a metal, ligand(s), a growing polymer chain, a coordinated olefin and a co-catalyst (activator), as depicted in Fig. 2.

In the course of investigations into polymerization catalysis of zirconocene catalysts for ethylene and propylene polymerizations, we noticed that catalysts with Cp-based ligands (Cp: cyclopentadienyl) having wider π-conjugation systems such as indenyl, fluorenyl and phenyl Cp usually display higher activities; namely, the higher activity catalysts generally possess a small energy gap between HOMO (highest occupied molecular orbital) and LUMO (lowest unoccupied molecular orbital) of the ligand. These results suggest that the electronic properties of ligands play a significant role in managing catalytic activity.

To gain further insight into the effect of the electronic nature of a ligand, DFT calculations were performed on a model metallocene catalyst (H$_2$SiCp$_2$ZrMe$^+$) for ethylene polymerization. The results demonstrate that ethylene polymerization is a process involving intense electron exchange between a metal and a ligand, probably to reduce the energy increase during the course of the polymerization. This fact
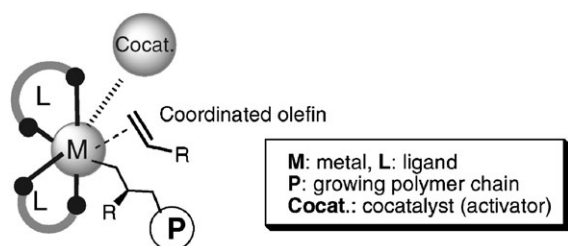

Fig. 2 A schematic structure of a molecular catalyst for olefin polymerization.

This journal is © The Royal Society of Chemistry 2008

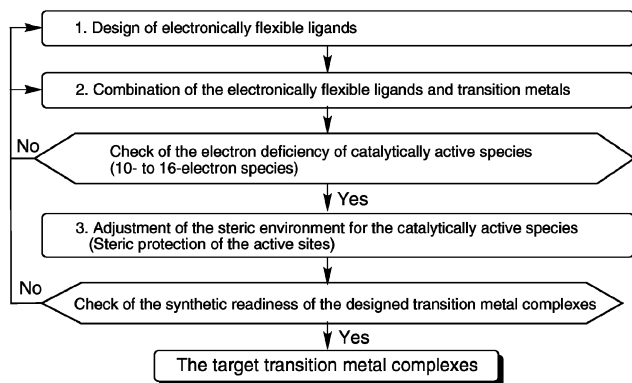*Chem. Soc. Rev.*, 2008, **37**, 1264–1277 | 1265

Fig. 3 Catalyst design procedures for the development of highly active catalysts.

suggests, that in order to achieve high activity, ligands must be electronically flexible enough to receive electrons from the coordinated olefin through a metal and to release electrons whenever it is needed to expedite the olefin insertion process. We believe that this is potentially achieved by a ligand that possesses a small energy gap between HOMO and LUMO.

With respect to metal selection, we decided to utilize both early and late transition metals such as Ti, Zr, Co and Ni, since all transition metals (even Mn and Fe) inherently possess olefin insertion ability. We thus postulate that it is the ligands that play the predominant role in controlling polymerization activity among the typical components of the catalyst. Therefore, we believe that the combination of a transition metal and electronically flexible ligand(s) can yield a highly active ethylene polymerization catalyst when activated as long as the potentially active species possesses an appropriate electron deficiency (*i.e.*, electrophilicity) as well as a pair of available *cis*-located sites for efficient polymerization. We have given the name "ligand oriented catalyst design concept" to the concept that attaches great importance to the electronically flexible properties of the ligand.[11–15]

Because transition metal complexes bearing non-symmetric ligands had been less extensively studied as olefin polymerization catalysts when we initiated this research, we have primarily focused on non-symmetric ligands that possess an electronically flexible nature. We anticipated that such ligands might form non-symmetric polymerization sites depending on the coordination modes of the ligands, leading to the generation of unique microstructure polymers. Altogether, transition metal complexes incorporating non-symmetric ligands that have electronically flexible properties were considered to be new and viable catalysts for olefin polymerization. Fig. 3 displays our catalyst design procedures for developing highly active catalysts.

3 Discovery of highly active catalysts

Examples of the designed ligands are summarized in Fig. 4, which includes neutral monoanionic as well as dianionic ligands. The ligands are non-symmetric and possess HOMO/LUMO energy gap values; <8.5 eV for neutral ligands and <7.0 eV for anionic ligands, at the MNDO-PM3 level calculations.

According to our ligand oriented catalyst design concept, we combined the electronically flexible ligands such as those shown in Fig. 4 with transition metals to obtain high-activity catalysts. We aimed at transition metal complexes that form 10- to 16-electron species, when activated. The synthesized complexes were investigated to determine their potential as ethylene polymerization catalysts with methylaluminoxane (MAO) activation at 25 °C under atmospheric pressure. As a result, we found a number of highly active ethylene polymerization catalysts containing electronically flexible [N, N], [N⁻, N], [O⁻, O], [O⁻, N], [Cp⁻, O⁻] or [O⁻, N, N] chelate ligands.[11–18]

Fig. 5 displays examples of newly discovered catalysts, which include pyrrolide-imine ligated group 4 transition metal complexes (PI catalysts),[39,58–61] indolide-imine ligated Ti complexes (II catalysts),[38,62] phenoxy-ether ligated Ti complexes (FE catalysts),[63] phenoxy-imine ligated early transition metal complexes (FI catalysts),[64–66] imine-phenoxy ligated Ti and Zr complexes (IF catalysts)[67,68] and phenoxy-pyridine ligated Ti complexes (FP catalysts).[69] The names of these catalysts are derived from the Japanese pronunciation of the ligands since these catalysts were discovered on the basis of the ligand oriented catalyst design concept. In the following section, we describe the catalytic performance of PI, II, FE, FI, IF and FP catalysts for olefin polymerization in an attempt to introduce their unique catalysis and distinctive polymer formation.
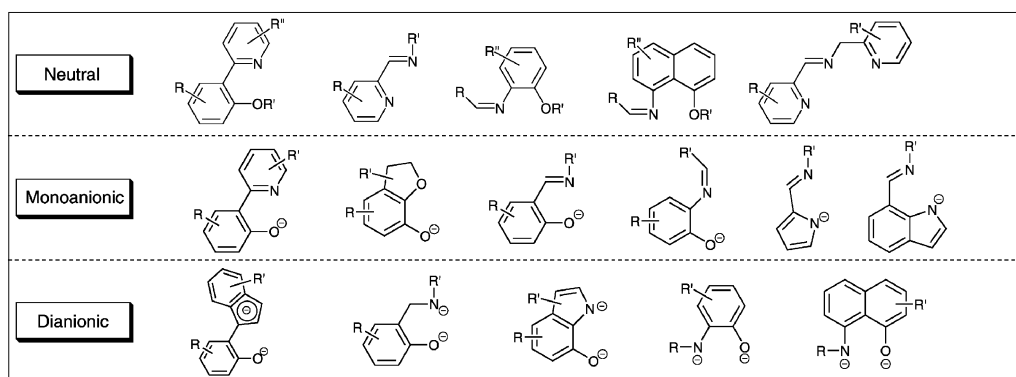

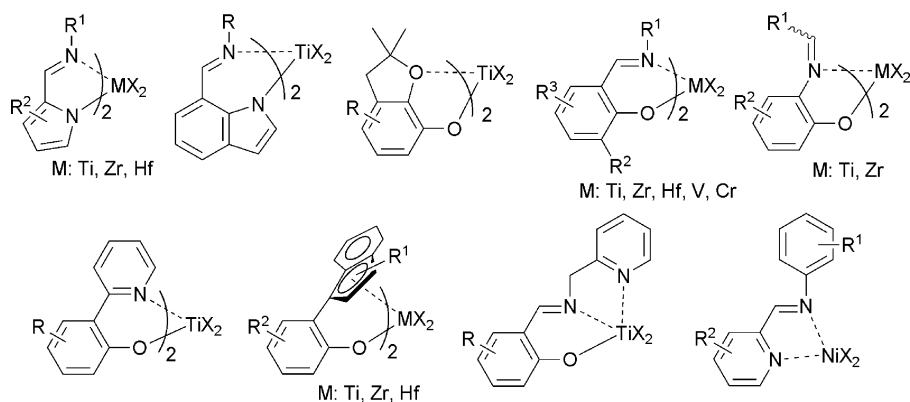**Fig. 4** Examples of the designed ligands.

Fig. 5 Highly active catalysts that were discovered on the basis of the ligand-oriented catalyst design concept.

4 Catalytic performance of the discovered catalysts

4.1 Pyrrolide-imine ligated group 4 transition metal complexes: PI catalysts

The olefin polymerization behavior of Ti complexes bearing pyrrolide-imine [N⁻, N] chelate ligands **1–6** (**1**: R = Ph, **2**: R = Et, **3**: R = n-C$_6$H$_{11}$, **4**: R = cyclohexyl, **5**: R = 4-t-Bu-cyclohexyl, **6**: R = cyclooctyl) (PI catalysts, Fig. 6) is introduced.[39,58–61]

The catalyst name "PI" comes from the Japanese pronunciation of the ligand "*Pirorido-Imin*". X-ray crystallographic analyses demonstrated that PI catalysts **1**, **2** and **4** contain approximately octahedrally coordinated Ti centers with mutually *trans* pyrrolide-nitrogens, *cis* imine-nitrogens and *cis* chlorines (*e.g.*, **4**, Fig. 7).[59]

Under the assumption that two chlorine-bound sites are transformed into olefin polymerization sites while retaining their *cis* relationship, active species stemming from these PI catalysts would possess a pair of *cis*-located polymerization sites, which are located *trans* to the neutral imine-nitrogens. Such a stereochemical structure is suggested by DFT calculations performed on ethylene-coordinated cationic methyl complexes (initial active species). Additionally, DFT calculations also indicate that the Ti center of a cationic methyl species derived from PI catalysts possess higher electrophilicity than those from Cp$_2$TiCl$_2$ and Me$_2$Si(Me$_4$Cp)(N-t-Bu)TiCl$_2$ (CGC) [Mulliken charge of the Ti in atomic units: 1.84 (from **4**), 1.31 (from Cp$_2$TiCl$_2$), 1.69 (from CGC)].[14,39]

When activated with MAO at 25 °C, PI catalysts **1–6** exhibit very high activities for ethylene polymerization, and produce highly linear PEs with high-molecular weights (M_v 75 000–3 167 000) (Table 1). The basic trend observed is that an increase in the steric bulk of the substituent on the imine-
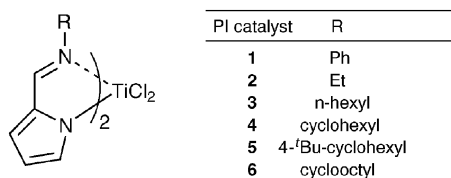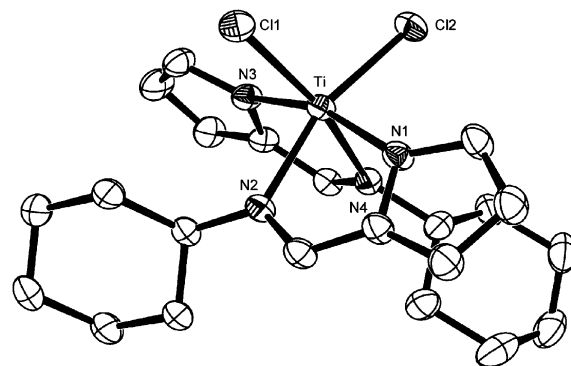

Fig. 7 Molecular structure of PI catalyst **4**. Hydrogen atoms are omitted.

nitrogen results in enhanced catalytic activity and the production of higher molecular weight PEs.

It is reasonable to think that the sterically more encumbered substituent gives better steric protection to the imine-nitrogen from Lewis acidic compounds present in a polymerization medium and, additionally, induces more efficient ion separation between the cationic active species and an anionic activator species. Moreover, the substituent reduces the rate of chain transfer more significantly than that of chain propagation.

The highest activity (33.2 kg-PE (mmol-cat h)$^{-1}$) obtained with PI catalyst **6** with MAO exceeds that for early group 4

Fig. 6 Structures of PI catalysts **1–6**.

Table 1 Ethylene polymerization results with PI catalysts **1–6**, Cp$_2$TiCl$_2$ and Cp$_2$ZrCl$_2$/MAO

Entry	PI catalyst	Activity^a	$10^{-3}M_v{}^b$
1	**1**	6.0	75
2	**2**	0.36	412
3	**3**	0.78	441
4	**4**	14.1	2601
5	**5**	20.4	2720
6	**6**	33.2	3167
7	Cp$_2$TiCl$_2$	16.7	1253
8	Cp$_2$ZrCl$_2$	20.0	1000

Conditions: 25 °C, atmospheric pressure, ethylene gas feed 100 l h^{-1}, complex: 1 mmol, MAO 1.25 mmol as Al, toluene 250 ml. ^{a} kg-polymer (mmol-cat h)$^{-1}$. ^{b} Calculated from intrinsic viscosity.

7: M=Zr (Zr-PI catalyst)
8: M=Hf (Hf-PI catalyst)

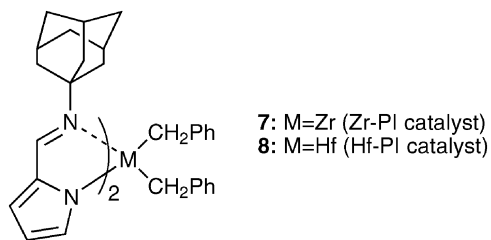**Fig. 8** Structures of Zr–PI and Hf–PI catalysts **7** and **8**.

metallocenes under identical conditions (Cp$_2$MCl$_2$, M = Ti: 16.7 kg-PE (mmol-cat h)$^{-1}$, M = Zr: 20.0 kg-PE (mmol-cat h)$^{-1}$), and represents one of the best reported activities for Ti-based catalysts under atmospheric pressure conditions. It is interesting to note that PI catalyst **4** with MAO possesses characteristics of living ethylene polymerization, though under limited conditions, and gives high-molecular-weight PEs with extremely narrow molecular weight distributions (M_n 225 000, M_w/M_n 1.15, 10-s polymerization, 25 °C). Aside from Ti–PI catalysts, Zr– and Hf–PI catalysts can be high-activity catalysts for ethylene polymerization. For example, Zr–PI catalyst **7** and Hf–PI catalyst **8** (Fig. 8) with MAO activation at 25 °C demonstrate very high activities of 22.9 and 2.1 kg-PE (mmol-cat h)$^{-1}$, respectively.[70,71]

It should be pointed out that PI catalysts **1–6** combined with *i*-Bu$_3$Al/Ph$_3$CB(C$_6$F$_5$)$_4$ convert ethylene to extremely high molecular weight PEs ($M_v > 4\,000\,000$) with high efficiency (>1.5 kg-PE (mmol-cat h)$^{-1}$). The molecular weights ($M_v > 4\,000\,000$) are some of the highest values encountered in homogeneous olefin polymerization catalysts. We attribute the production of these ultra-high molecular weight PEs to a pyrrolide-amine ligated Ti complex with a *i*-Bu$_2$Al group attached to the amine-donor that is generated as a result of the reduction of the imine moiety by *i*-Bu$_3$Al (and its contaminant *i*-Bu$_2$AlH) with the concurrent formation of isobutene (Fig. 9). A similar imine-reduction is also observed for group 4 transition metal complexes that contain phenoxy-imine chelate ligands (FI catalysts and IF catalysts),[67,68,75,76] suggesting that such a reduction is not unusual though little has been reported about the reduction of free imine functionality with *i*-Bu$_3$Al.

Encouraged by the high-ethylene polymerization activity together with the highly electrophilic nature of the catalytically active species (which is suggested by DFT calculations), we turned our attention to the copolymerization of ethylene and norbornene (NB). This is because NB has high nucleophilicity relative to ethylene and α-olefins (as indicated by high HOMO energy level, NB: −7.25 eV, ethylene: −8.15 eV, propylene: −7.66 eV, DFT calculations) and thus exhibits high affinity to
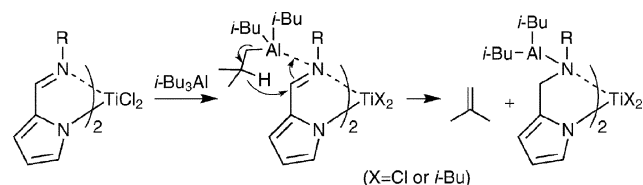

Fig. 9 Reaction scheme for the formation of a pyrrolide–amine complex.

Table 2 Ethylene/NB copolymerization results with PI catalysts **1**, **4**, **5** and **6**/MAO

Entry	PI catalyst	Activity[a]	$10^{-3}M_n$[b]	M_w/M_n[b]	T_g[c]/°C
1	**1**	2.73	521	1.16	120
2	**4**	0.58	127	1.10	130
3	**5**	2.15	417	1.24	121
4	**6**	3.19	600	1.23	126

Conditions: 25 °C, atmospheric pressure, 10 min, ethylene gas feed 50 l h^{-1}, NB (charged) 10 g. Complex: 1 mmol, MAO 1.25 mmol as Al, toluene 250 ml. [a] kg-polymer (mmol-cat h)$^{-1}$. [b] M_n and M_w/M_n values were determined by GPC equipped with refractive index (RI) detector. [c] Measured by DSC.

highly electrophilic active species originating from PI catalysts.[14,39] Ethylene/NB copolymers are known to have high thermal stability and excellent optical properties, and are thus used in heat-resistant and optical applications.

On activation with MAO at 25 °C, PI catalysts **1**, **4**, **5** and **6** show very high incorporation ability for NB and furnish copolymers with high NB contents (and thus with high T_g's; T_g correlates with NB content) (Table 2). The NB contents and T_g's obtained with these PI catalysts are higher than those for CGCs, which are well-known to exhibit very high incorporation of sterically encumbered monomers.

The highly electrophilic nature of the active species is probably responsible for the high incorporation ability for NB. The catalysts exhibit a marked tendency to form alternating copolymers, which have stereoirregular structures despite the C_2-symmetric nature of the catalysts. An interesting dependence of molecular weight distribution on the molar ratio of NB to ethylene in the polymerization medium was observed. At NB/ethylene ratios larger than *ca.* 1, PI catalysts **1**, **4**, **5** and **6** with MAO promote the room-temperature living copolymerization of ethylene and NB to yield very high molecular weight copolymers with extremely narrow molecular weight distributions ($M_n > 500\,000$, $M_w/M_n < 1.20$). Living nature was further confirmed by the fact that copolymerizations catalyzed by these PI catalysts with MAO exhibit a linear increase of M_n with polymerization time.

Interestingly, characterization of the resultant copolymers by ^{13}C NMR spectroscopy revealed that the chain-end structures of the copolymers are consistent with chain initiation by insertion of NB into the Ti–Me bond, and a last-inserted NB unit after termination by protonolysis. Polymerization results coupled with DFT calculations suggested that the highly controlled living polymerization originates from the fact that the catalysts possess high affinity and high-incorporation ability for NB as well as some characteristics of a living ethylene polymerization. NB probably plays a key role in stabilizing the active species against chain termination *via* β-H transfer and chain transfer to Al, which is also indicated by DFT calculations.[14,39]

The unique living nature allows the first synthesis of the block copolymers consisting of poly(ethylene-*co*-NB) segments with varying degrees of NB incorporation as well as the block copolymers containing PE and poly(ethylene-*co*-NB) segments. TEM imaging of PE-*b*-poly(ethylene-*co*-NB) (M_n 414 000, M_w/M_n 1.56, overall NB content 31 mol%)
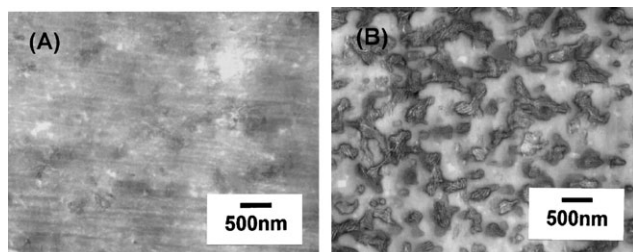
Fig. 10 TEM micrographs of (A) PE-*b*-poly(ethylene-*co*-NB) and (B) PE and poly(ethylene-*co*-NB) blend polymer.

reveals a homogeneous morphology whereas the corresponding blend polymer reveals significant inhomogeneity because of phase separation (Fig. 10), indicating that the block copolymer possesses high potential as a new material comprised of crystalline and amorphous segments that are chemically linked.

4.2 Indolide-imine ligated Ti complexes: II catalysts

In addition to PI catalysts that contain [N⁻, N] ligands, Ti complexes featuring indolide-imine [N⁻, N] chelate ligands 9–12 (9: R = Ph, 10: R = 2,6-difluorophenyl, 11: R = 2,4,6-trifluorophenyl, 12: R = pentafluorophenyl) (II catalysts, Fig. 11) exhibit unique catalysis for olefin polymerization.[38,62]

The catalyst name "II" stems from the Japanese pronunciation of the ligand "*Indorido-Imin*". While we do not have X-ray analysis data for II catalysts, DFT calculations indicate that II catalysts 9–12 contain approximately octahedrally coordinated Ti centers with mutually *trans* indolide-nitrogens, *cis* imine-nitrogens and *cis* chlorines. The calculations also suggest that cationic methyl species derived from these II catalysts possess *cis*-located sites for polymerization; a methyl group and a coordinated ethylene are in a *cis* configuration and are *trans* to the neutral imine-nitrogens (*e.g.*, 9, Fig. 12).[38]

II Catalysts 9–12 in combination with MAO at 25 °C form active catalysts for the polymerization of ethylene. It can be seen from Table 3 that the catalytic activity shows a marked dependency on the number of fluorine atoms in the ligand.

The basic trend observed is that an increase in the number of fluorine atoms in the II ligand results in increased catalytic activity. These results provide the first clear demonstration that the electrophilicity of the metal center in active species plays a predominant role in determining catalytic activity, unlike group 4 metallocene catalysts whose activity is decreased by the introduction of electron-withdrawing substituent(s) in Cp ligands. The same trend was observed for FI catalysts.[73,74] It is reasonable to assume that a more electrophilic Ti center, which is generated by a more electron-withdrawing ligand, results in an increase in metal-carbon
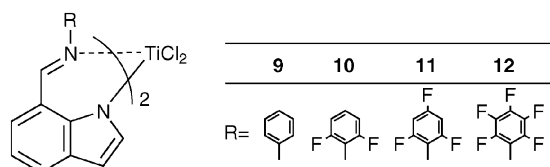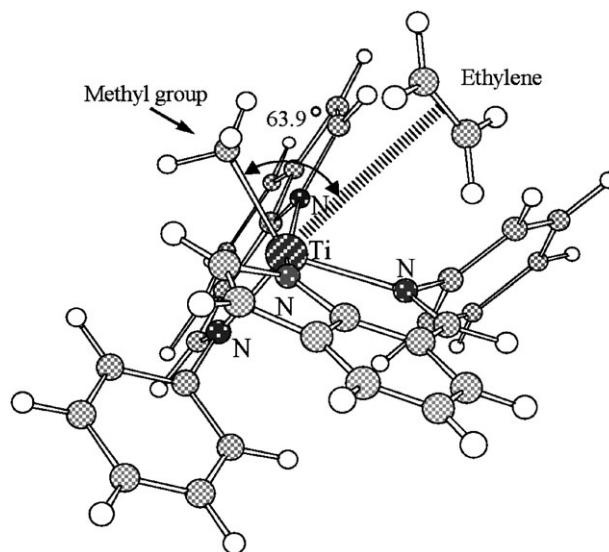

Fig. 12 Calculated structure of an ethylene-coordinated cationic methyl species generated from II catalyst 9.

reactivity, leading to reduced activation energy for ethylene insertion.

The activity obtained with II catalyst 12/MAO (1.14 kg-PE (mmol-cat h)⁻¹) is comparable to that seen with the highly active Ti complex incorporating a pair of phosphinimide ligands reported by Stephan (1.17 kg-PE (mmol-cat h)⁻¹, 25 °C).[8]

II catalysts 9–12 in conjunction with MAO produce highly linear PEs having moderate to high molecular weights (M_w 13 800–323 000). GPC analyses demonstrated that the PEs formed with II catalysts 9–11 possess extremely narrow molecular weight distributions (M_w/M_n 1.11–1.14) whereas that produced with 12 has an M_w/M_n of 1.93. Additionally, the polymerizations with II catalysts 9–11 exhibit a linear increase in M_n with PE yield, indicating living ethylene polymerization. These are rare examples of living ethylene polymerization at room temperature.[36,37] It is noteworthy that II catalyst 11/MAO shows impressive thermal stability in that the PE formed at 50 °C retains a narrow molecular weight distribution of 1.24.

While II catalyst 12/MAO produces PE with a broadened molecular weight distribution relative to the PEs arising from II catalysts 9–11/MAO at 25 °C, experimental results indicate that the polymerization proceeds without β-H transfer and chain transfer to Al. In addition, the experimental results also

Fig. 11 Structures of II catalysts 9–12.

Table 3 Ethylene polymerization results with II catalysts 9–12

Entry	II Catalyst	Activity[a]	$10^{-3}M_w$[b]	M_w/M_n[b]
1	9	0.05	14	1.14
2	10	0.06	12	1.13
3	11	0.29	47	1.11
4	12	1.14	323	1.93

Conditions: 25 °C, atmospheric pressure, 10 min, ethylene gas feed 100 l h⁻¹, complex: 5.0 μmol, MAO 1.25 mmol as Al, toluene 250 ml. [a] kg-polymer (mmol-cat h)⁻¹. [b] M_n and M_w/M_n values were determined by GPC.
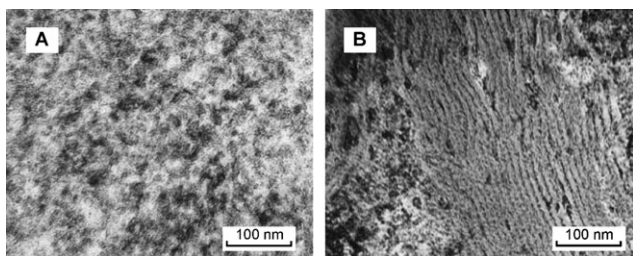
Fig. 13 TEM micrographs of (A) PE-*b*-poly(ethylene-*co*-propylene) and (B) polyethylene and poly(ethylene-*co*-propylene) blend polymer.

suggest that some catalyst deactivation is involved in the polymerization process. As expected, upon lowering the polymerization temperature to -10 °C, II catalyst **12**/MAO mediates living ethylene polymerization to furnish PEs with extremely narrow molecular weight distributions (M_w/M_n 1.12–1.25). The catalytic activity obtained at -10 °C (1.94 kg-PE (mmol-cat h)$^{-1}$) is much higher than that at 25 °C (1.14 kg-PE (mmol-cat h)$^{-1}$), indicative of the catalyst deactivation at a higher temperature.

Since II catalyst **9** having no fluorine in the ligand, on activation with MAO, inserts ethylene in a living fashion, the achievement of the living polymerization with II catalysts is mainly attributed to the bulky and rigid II ligand. Recent research using DFT calculations, however, suggest that there is an attractive interaction between the *ortho*-fluorine and a β-H on a growing polymer chain though the interaction is weaker than that calculated for fluorinated Ti–FI catalysts, which will be described elsewhere.

Living behavior of II catalysts/MAO was exemplified through the synthesis of PE-*b*-poly(ethylene-*co*-propylene) that was comprised of crystalline and amorphous segments. The T_m of the block copolymer (127 °C) is only a few degrees lower than that of the homopolymer (PE), suggesting that the block copolymer displays good elastic properties at much higher temperatures than the conventional random copolymers of similar density. The TEM imaging of the block copolymer (M_n 31400, M_w/M_n 1.17, overall propylene content 8 mol%) revealed microphase separation of the poly(ethylene-*co*-propylene) and PE domains, which are evenly dispersed throughout the sample, which lies in sharp contrast to the case of the corresponding blend polymer (Fig. 13).[38]

4.3 Phenoxy-ether ligated Ti complexes: FE catalysts

The catalytic behavior of Ti complexes bearing phenoxy-ether [O$^-$, O] chelating ligands **13** and **14** (**13**: R = *t*-Bu, **14**: R = 1-adamantyl) (FE catalysts, Fig. 14) is discussed for the polymerization of ethylene.[63]
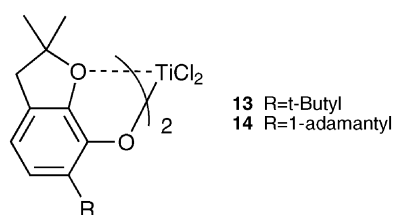

Fig. 14 Structures of FE catalysts **13** and **14**.
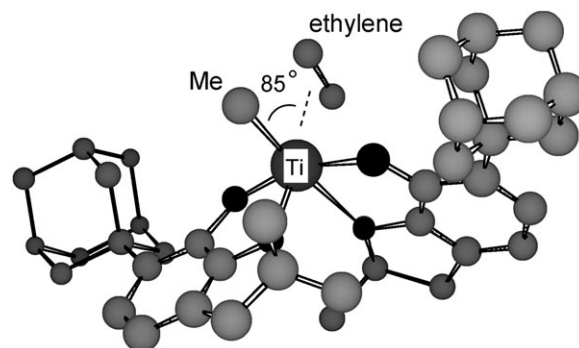

Fig. 15 Calculated structure of an ethylene-coordinated cationic methyl species generated from FE catalyst **14**.

The catalyst name "FE" was given after the Japanese pronunciation of the ligand "*Fenokishi-Eteru*". DFT calculation studies suggest that ethylene-coordinated cationic methyl species derived from FE catalysts **13** and **14** assume an octahedral geometry with *trans*-phenoxy-oxygens, *cis*-ether-oxygens and the *cis*-Me/coordinated-ethylene disposition, indicative of the *cis*-located polymerization sites that are situated *trans* to the neutral ether-oxygens (Fig. 15).

Treatment of FE catalysts **13** and **14** with MAO or *i*-Bu$_3$Al/Ph$_3$CB(C$_6$F$_5$)$_4$ at 25 °C yield active catalysts for the polymerization of ethylene (Table 4). All of the catalyst systems convert ethylene to highly linear PEs having very high molecular weights (M_v 2 040 000–5 420 000) with high efficiency (0.27–3.47 kg-PE (mmol-cat h)$^{-1}$), representing rare examples of highly active Ti-based catalysts featuring monoanionic bidentate [O$^-$, O] chelating ligand(s).

FE catalyst **13** bearing an adamantly group *ortho* to the phenoxy-oxygen displays higher activity than FE catalyst **14** with a *t*-Bu group at the same position. Similar beneficial effects of sterically encumbered substituents in close proximity to the active sites were observed for PI catalysts and FI catalysts.[39,59,75] The highest activity obtained with FE catalyst **14**/*i*-Bu$_3$Al/Ph$_3$CB(C$_6$F$_5$)$_4$ (3.47 kg-PE (mmol-cat h)$^{-1}$) compares favorably with that of Ti–FI catalyst **24** (Fig. 18)/MAO (2.9 kg-PE (mmol-cat h)$^{-1}$), and is one of the best reported activities for Ti-based non-metallocene catalysts under analogous conditions.[63]

FE catalyst **13**/MAO forms PE with an extremely high molecular weight (M_v 5 420 000), which is one of the highest molecular weights obtained with molecular catalysts. FE catalyst **14**, which possesses the sterically larger *ortho* substituent, furnishes lower (but still very high) molecular weight PE

Table 4 Ethylene polymerization results with FE catalysts **13** and **14**

Entry	FE catalyst	Co-catalyst	Activity[a]	$M_v (\times 10^4)$
1	**13**	MAO	0.27	542
2	**13**	Borate	1.45	312
3	**14**	MAO	2.82	204
4	**14**	Borate	3.47	260

Conditions: 25 °C, atmospheric pressure, 10 min, ethylene gas feed 100 l h^{-1}, complex: 5.0 µmol, MAO 1.25 mmol as Al, borate (Ph$_3$CB(C$_6$F$_5$)$_4$ 6 µmol, *i*-Bu$_3$Al 50 µmol, toluene 250 ml. [a] kg-polymer (mmol-cat h)$^{-1}$.

Fig. 16 Structures of FI catalysts **15** and **16**.

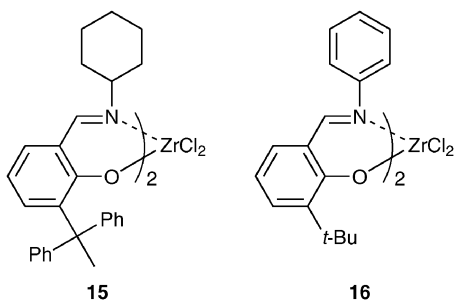| FI catalyst	R^1	R^2
17	cyclopropyl	H
18	cyclobutyl	H
19	cyclobutyl	Me
20	cyclopentyl	H
21	cyclohexyl	H
22	2-isopropylphenyl	H

Fig. 17 Structures of FI catalysts **17–22**.

than FE catalyst **13**, which is rather unexpected. Considering that molecular weight is determined by the relative rates of chain propagation and chain transfer, in this case the sterically encumbered group *ortho* to the phenoxy-oxygen influences the rate of chain propagation more significantly than that of chain transfer.

4.4 Phenoxy-imine ligated early transition metal complexes: FI catalysts

Among the high-activity catalysts that have so far been discovered on the basis of the ligand oriented catalyst design concept, bis(phenoxy-imine) early transition metal complexes (FI catalysts, Fig. 16; the catalyst name "FI" comes from the Japanese pronunciation of the ligand "*Fenokishi-Imin*") display strikingly high activity when activated with MAO. The activities in many cases are higher than those obtained from group 4 metallocene catalysts under analogous conditions. The highest activity displayed by FI catalyst **15** (Fig. 16) reached an astonishing value of 6552 kg-PE (mmol-cat h)$^{-1}$ under atmospheric pressure conditions at 25 °C.[11–13,72–74] This activity corresponds to a catalyst turnover frequency (TOF) of 64 900 s^{-1} atm^{-1}, which is two orders of magnitude greater than that for Cp$_2$ZrCl$_2$ with MAO. To the best of the authors' knowledge, this TOF is probably the largest recorded, not only for olefin polymerization, but for any other catalytic reaction.

DFT calculations suggest that a cationic methyl complex derived from an FI catalyst normally possesses a pair of *cis*-located polymerization sites, which are situated *trans* to the imine-nitrogens. Additionally, the calculations performed on FI catalyst **16** (Fig. 16) indicate that the Zr–N bonds that lie on the same plane as polymerization sites expand and contract according to the reaction coordinate of the ethylene insertion (2.23–2.34 Å), whereas the Zr–O bond length remains virtually constant. We postulate that the electronically flexible nature of the FI ligands and the *cis*-located polymerization sites as well as this variable Zr–N bond length (which facilitates a smooth and flexible electron exchange between the metal and the ligands) are responsible for the high-polymerization activities of FI catalysts.[75]

The very high catalyst efficiency and readily varied steric as well as electronic properties of the phenoxy-imine ligands of FI catalysts have afforded a wide variety of polyolefinic materials, some of which were previously unavailable through other means of polymerization.[11–15] The materials include ultra-high-molecular-weight PEs,[75,76] ethylene/α-olefin copolymers and atactic PPs,[24,28] well-defined and controlled multi-
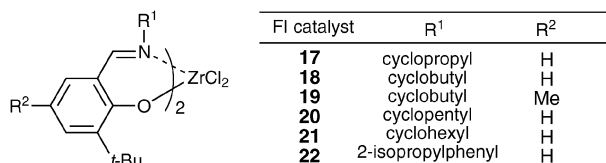
modal PEs,[22,23] selective vinyl- and Al-terminated PEs,[19–21] and ultra-fine non-coherent particle PEs with ultra-high molecular weights.[15,77–79] In addition, FI catalysts can produce highly isotactic and syndiotactic PPs with exceptionally high T_m's,[28–33] and stereo- and regioirregular high-molecular-weight poly(higher α-olefin)s.[25,27] Moreover, FI catalysts allow access to ethylene and/or propylene-based telechelic polymers[80] and di- and multi-block copolymers from ethylene, propylene and higher α-olefins.[33–37] In this section, the preparations of selective vinyl- and Al-terminated PEs, stereo- and regioirregular high-molecular-weight poly(higher α-olefin)s and polyolefinic block copolymers using FI catalysts are introduced. For the syntheses of other polymers with FI catalysts, the reader is referred to the reviews and original papers that are summarized in refs. 11–15, 22–24, 28–32 and 75–81.

4.4.1 Vinyl- and Al-terminated PEs. On activation with MAO, Zr–FI catalysts bearing phenoxy-cycloalkylimine ligands are capable of forming low-molecular-weight PEs having a high degree of vinyl unsaturation at one of the two polymer chain-ends, with high efficiency.[19,20] For instance, at 25 °C FI catalysts **17–21** (Fig. 17) convert ethylene to yield vinyl-terminated low molecular weight PEs (M_w 2000–14 000, vinyl selectivity 90–96%) with higher activities than Cp$_2$ZrCl$_2$/MAO (28 kg-PE (mmol-cat h)$^{-1}$) under identical conditions (Table 5).

These are the first examples of group 4 metal-based catalysts that produce vinyl-terminated low-molecular-weight PEs with high productivity at ambient temperatures. The vinyl-terminated low-molecular-weight PEs can be transformed by chain-end functionalization to produce end-functionalized PEs that are valuable materials for block and graft copolymers containing a PE and a polar polymer segment. In fact, the vinyl-terminated PEs are readily transformed to the corresponding epoxy-PEs by H$_2$O$_2$ oxidation and diol-terminated PEs by subsequent hydrolysis,[20] allowing the creation of PE/polyethylene glycol block copolymers and polyesters with PE branches.

Table 5 Ethylene polymerization results with FI catalysts **17–21**

Entry	FI catalyst	Activity^a	$10^{-3}M_w{}^b$	$M_w/M_n{}^b$	Vinyl end^c (%)
1	**17**	50.4	4.4	2.0	91
2	**18**	31.6	2.0	1.7	95
3	**19**	22.0	2.0	1.7	94
4	**20**	67.2	3.6	2.1	96
5	**21**	87.7	14	1.7	90

Conditions: 25 °C, atmospheric pressure, 5 min, ethylene gas feed 100 l h^{-1}, complex: 0.5 μmol, MAO 0.625 mmol as Al, toluene 250 ml. ^{a} kg-polymer (mmol-cat h)$^{-1}$. ^{b} M_w and M_w/M_n values were determined by GPC. ^{c} Degree of vinyl unsaturation at one of the two polymer chain ends, determined by ^{1}H NMR.

Table 6 Ethylene polymerization results for FI catalysts 17 and 22 with MAO or MAO/trimethylaluminium (TMA)

Entry	FI catalyst	MAO/mmol	TMA/mmol	Al/Zr	Activity[a]	$10^{-3} M_w$[b]	M_w/M_n[b]	V/M[c]
1	**16**	1.250	0	2500	116	9	2.4	47/53
2	**22**	1.250	0	2500	66	90	2.0	0/100
3	**22**	0.625	0	1250	66	159	2.3	0/100
4	**22**	0.250	0	500	58	716	2.6	0/100
5	**22**	0.250	3.5	7500	34	12	2.0	0/100
6[d]	**22**	0.250	0.20	900	41	201	5.9	0/100

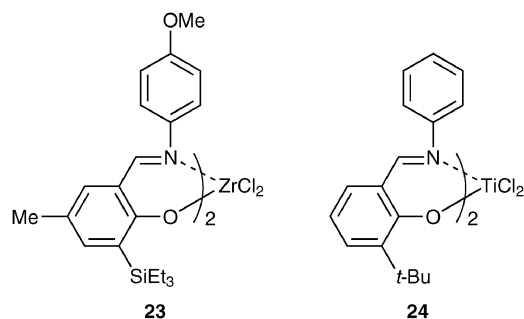*Conditions*: 25 °C, atmospheric pressure, 5 min ([d]30 min), ethylene gas feed 100 l h^{-1}, complex: 0.5 μmol. [a] kg-polymer (mmol-cat h)$^{-1}$. [b] Determined by GPC. [c] Chain-end group: vinyl/methyl (molar ratio).

Ethylene pressure studies demonstrated a first-order dependence on ethylene for both the rate of chain propagation and the rate of chain transfer. This polymerization behavior along with X-ray analyses and DFT calculation studies provided strong support for β-H transfer to an incoming monomer, which is responsible for the formation of vinyl-terminated PEs. The calculations suggested that the catalysts disfavor β-H transfer to the Zr metal due to the extreme instability of a metal hydride species that is produced in such a chain transfer process.

Conversely and interestingly, we revealed that Zr–FI catalyst 22 (Fig. 17) incorporating a 2-isopropylphenyl group on the imine-N in conjunction with MAO or MAO plus trimethylaluminium displays a marked preference for chain transfer to aluminum and quantitatively produces Al-terminated PEs having low-to-very-high molecular weights and narrow-to-broad molecular weight distributions with high efficiency (Table 6).[21]

The isopropyl group discourages β-H transfer, resulting in the exclusive formation of Al-terminated polymers. With established methods, the Al-PEs can readily be transformed to a variety of functionalized PEs and PE- and polar polymer-based block and graft copolymers. The selective synthesis of vinyl- and Al-terminated PEs with Zr–FI catalysts indicates the critical importance of the substituent on the imine-nitrogen for polymerization catalysis.

4.4.2 Stereo- and regioirregular high-molecular-weight poly(higher α-olefin)s.
A unique feature of FI catalysis is that FI catalysts on activation with *i*-Bu₃Al /Ph₃CB(C₆F₅)₄ furnish ultra-high molecular weight (co)polymers, unlike the situation with MAO activation.[24,28,75,76] For example, Zr–FI catalyst 16 (Fig. 16) with this activation system forms PE with an exceptionally high-molecular weight (M_v) of above 5 000 000, though with MAO activation, molecular weight (M_w) is merely 10 000.[75] Additionally, Zr–FI catalyst 23 (Fig. 18) in association with *i*-Bu₃Al/Ph₃CB(C₆F₅)₄ at 70 °C, under 0.9 MPa ethylene–propylene total pressure, produces an amorphous ethylene/propylene copolymer (propylene content 20 mol%) with an exceptionally high molecular weight (M_w) of 10 200 000 (M_w/M_n 2.52), and a very high activity of 36 kg-polymer (mmol-cat h)$^{-1}$.[24] The molecular weight probably represents the highest molecular weight known to date for a linear, synthetic copolymer.

NMR studies together with experimental results suggest that a catalytically active species generated from an FI catalyst with *i*-Bu₃Al/Ph₃CB(C₆F₅)₄ is a phenoxy-amine complex with *i*-Bu₂Al attached to the amine-nitrogen. Similar reductions are observed for PI and IF catalysts.[59,67,68]

A Ti–FI catalyst in combination with *i*-Bu₃Al/ Ph₃CB(C₆F₅)₄, which forms a phenoxy-amine Ti complex as a catalytically active species, displays unique behavior for the polymerization of higher α-olefins.[25–27] For example, Ti–FI catalyst 24 (Fig. 18) with *i*-Bu₃Al/Ph₃CB(C₆F₅)₄ exhibits high activities toward higher α-olefins (*i.e.*, 1-hexene, 1-octene, 1-decene, and 4-methyl-1-pentene) and produces high molecular weight polymers.

Surprisingly, the system showed higher activities toward higher α-olefins that incorporate more sterically-encumbered substituents in close proximity to the olefinic moieties. This is remarkable, because an olefin polymerization catalyst normally displays lower reactivity toward sterically-larger olefins due to steric hindrance. One explanation for this highly unusual behavior is that a sterically bulkier side chain originating from the last-inserted higher α-olefin of the growing polymer chain opens the phenoxy-amine ligands wider, thereby facilitating the coordination of the higher α-olefin to the metal and its insertion into the metal–carbon bond. Interestingly, DFT calculations suggest that one of the amine-donors is detached during the course of the polymerization of 1-hexene.

To our surprise, the polymerization rate has practically a zeroth-order dependence on the concentration of the monomer, which is a rare example for a group 4 metal-based catalyst. While the reason for the zeroth-order dependence is unclear at the current time, one possible explanation is that, under the conditions examined, the cationic complex virtually exists as a (higher α-olefin)-coordinated form, presumably due to the highly electrophilic as well as sterically-open nature of the cationic active species.[27]

Fig. 18 Structures of FI catalysts 23 and 24.

Table 7 Higher α-olefin polymerization results for FI catalyst **24** with i-Bu$_3$Al/Ph$_3$CB(C$_6$F$_5$)$_4$

Entry	Monomer	Activity[a]	$10^{-3} M_w$[b]	M_w/M_n[b]
1	1-Hexene	1.30	846	1.65
2	1-Octene	1.94	906	1.68
3	1-Decene	2.59	850	1.75
4	4MP[c]	3.00	1450	1.71

Conditions: 25 °C, atmospheric pressure, 20 min, monomer 0.211 mol, n-heptane 90 ml, pretreated solution of FI catalyst **24** (5 μmol)/ i-Bu$_3$Al (0.15 mmol), Ph$_3$CB(C$_6$F$_5$)$_4$ 6 μmol, i-Bu$_3$Al 50 μmol. [a] kg-polymer (mmol-cat h)$^{-1}$. [b] Determined by GPC. [c] 4-Methyl-1-pentene.

The resultant polymers have very high molecular weights [poly(1-hexene); M_w 846 000, M_w/M_n 1.65, poly(1-octene); M_w 906 000, M_w/M_n 1.68, poly(1-decene); M_w 850 000, M_w/M_n 1.75, poly(4-methyl-1-pentene); M_w 1 450 000, M_w/M_n 1.71], representing some of the highest reported for poly(higher α-olefin)s. Microstructural analyses using ^{13}C NMR spectroscopy has revealed that these high-molecular-weight polymers possess atactic structures with significant regio-irregular units (*ca.* 50 mol%) (stereo- and regio-irregular high-molecular-weight poly(higher α-olefin)s, "*ultra-random polymers*").[27] Considering that a 2,1-regio-error can have a detrimental effect on polymer molecular weights and normally encourages chain termination (which usually leads to low-molecular weights), the production of high- molecular-weight poly(higher α-olefin)s including frequent regio-errors is highly significant (Table 7).

4.4.3 Polyolefinic block copolymers. We have discovered that Ti–FI catalysts that incorporate fluorine(s) *ortho* to the imine-nitrogen can mediate highly controlled living ethylene and propylene polymerizations.[33–37,74,82–88] For example, Ti–FI catalyst **25** (Fig. 19) with MAO produces very high molecular weight monodisperse PEs with extremely high activities at 50 °C (M_w/M_n 1.13, M_n 424 000, TOF 21 500 min^{-1}·atm^{-1}).[82,85] This M_n value of 424 000 is one of the highest reported values to date for monodisperse PEs. To our surprise, at 90 °C, **25**/MAO furnishes PEs with fairly narrow molecular weight distributions (M_w/M_n 1.30, M_n 167 000).

Additionally, Ti–FI catalyst **26** (Fig. 19) combined with MAO at 25 °C, despite being C_2-symmetric in nature, affords highly syndiotactic monodisperse PP (rr 93%, M_n 47 000, M_w/M_n 1.08) with an exceptionally high T_m of 152 °C, which is one of the highest T_m's among sPPs synthesized at room temperature.[86–88] The syndioselective living polymerization

proceeds *via* a chain-end control mechanism with unusual 2,1-insertion.[86–91] Although chain-end control is operative in the polymerization, the stereoregularity is governed by the ligand structures, to which we have given the name "*ligand-directed chain-end controlled polymerization*".[11–15,34–37,86–88]

On the basis of theoretical calculations as well as well-established experimental results, we conclude that these unusual polymerization features of fluorinated Ti–FI catalysts originate from an attractive interaction between the *ortho*-F and a β-H on the growing polymer chain (living polymerization) and the fluxional character of the catalyst coupled with 2,1-regiochemistry (sPP formation with a C_2-symmetric catalyst).[32,35,36,85,87,88,92–94] This is in stark contrast to group 4 metallocene catalysts, which control olefin polymerization mainly by repulsive interactions based on the rigidly-organized ligand frameworks.

The versatile and robust living nature of the fluorinated Ti–FI catalysts allows for the preparation of a wide variety of unique block copolymers composed of crystalline and amorphous segments and/or two different kinds of crystalline segments; most of which were previously unavailable from Ziegler–Natta catalysis.[33–37] For example, FI catalyst **25** (Fig. 19) produces PE-*b*-poly(ethylene-*co*-propylene), PE-*b*-poly(ethylene-*co*-propylene)-*b*-PE, sPP-*b*-poly(ethylene-*co*-propylene), PE-*b*-sPP, and PE-*b*-poly(ethylene-*co*-propylene)-*b*-sPP.[85,95] Moreover, FI catalyst **27** (Fig. 19) forms ethylene/higher α-olefin block copolymers such as PE-*b*-poly(ethylene-*co*-1-hexene) and PE-*b*-poly(ethylene-*co*-1-octene).[96]

Recently, the elaborate FI-catalyst-design work that focuses on the substitution pattern of fluorine atoms as well as the substituent *ortho* to the phenoxy-oxygen has enabled us to achieve the catalytic production of living polymers including PE-*b*-poly(ethylene-*co*-propylene) in the presence of an appropriate chain transfer agent (*e.g.*, H$_2$, Et$_2$Zn).[34–36,97]

TEM visualization of sPP-*b*-poly(ethylene-*co*-propylene) (M_n 161 000, M_w/M_n 1.51, overall propylene content 40 mol%) revealed that this block copolymer exhibits a micro-phase-separated well-defined morphology with sPP domains (*ca.* 10 nm in diameter) embedded into the poly(ethylene-*co*-propylene) matrix (Fig. 20).[95] Additionally, AFM analysis revealed that PE-*b*-poly(ethylene-*co*-propylene) can exist as an individual molecule in which a PE lamella is covered with an amorphous ethylene/propylene copolymer segment.[98]

The block copolymers introduced herein display unique material properties; in particular, PE- or sPP- and amorphous ethylene/α-olefin copolymer-based block copolymers show excellent elastic properties at much higher temperatures than the conventional random copolymers of similar densities.

25: R=t-Bu
26: R=SiMe$_3$
27: R=Me
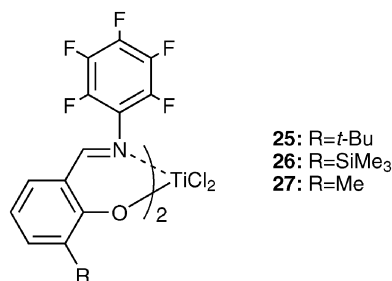
Fig. 19 Structures of FI catalysts **25–27**.
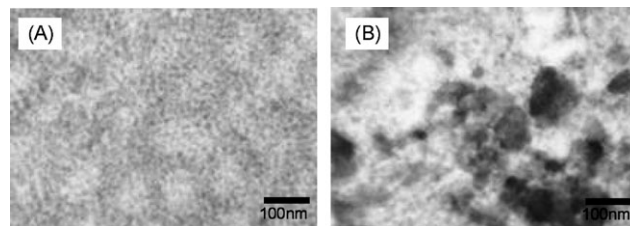
Fig. 20 TEM micrographs of (A) sPP-*b*-poly(ethylene-*co*-propylene) and (B) s-PP and poly(ethylene-*co*-propylene) blend polymer.
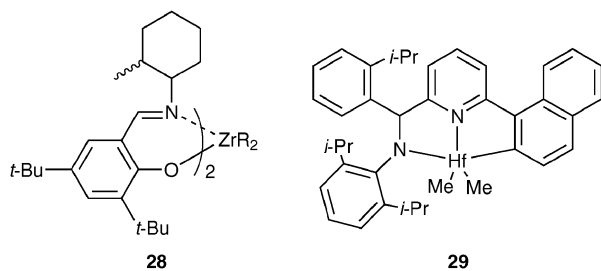
This journal is © The Royal Society of Chemistry 2008

Chem. Soc. Rev., 2008, **37**, 1264–1277 | 1273

Fig. 21   Structures of Zr–FI catalyst **28** and Hf complex **29**.

30 M = Ti, R = Ph
31 M = Ti, R = C_6F_5
32 M = Zr, R = Ph
33 M = Zr, R = C_6F_5

Fig. 22   Structures of IF catalysts **30–33**.

One of the notable additions of FI catalysis to block copolymer synthesis is the production of multi-block copolymers composed of PE and amorphous poly(ethylene-*co*-1-octene) segments, by a catalyst system comprised of Zr–FI catalyst **28**, Hf complex **29** (Fig. 21) and Et_2Zn, reported by researchers at Dow.[57] The Zr–FI catalyst selectively generates PE even in the co-presence of ethylene and 1-octene while the Hf complex produces amorphous copolymers, resulting in the formation of PE- and poly(ethylene-*co*-1-octene)-based multi-block copolymers through a reversible chain transfer reaction mediated by R_2Zn. The development of an FI catalyst with extremely high ethylene selectivity as well as the reversible chain transfer nature has made it possible to produce these unique polymers (Table 8).

4.5   Imine-phenoxy ligated Ti and Zr complexes: IF catalysts

The ethylene polymerization behavior of Ti and Zr complexes incorporating non-salicylaldimine-type (non-FI type) imine-phenoxy ligands **30–33** (**30**: M = Ti, R = Ph, **31**: M = Ti, R = pentafluorophenyl, **32**: M = Zr, R = Ph, **33**: M = Zr, R = pentafluorophenyl) is described (IF catalysts, Fig. 22; the catalyst name "IF" stems from the Japanese pronunciation of the ligand "*Imin-Fenokishi*").[67,68]

X-Ray crystal analysis of the adduct **30**·HCl has revealed that it exists as a zwitterionic complex, in which H and Cl are located in close proximity to one of the imine-nitrogens and Ti, respectively (Fig. 23). X-Ray crystallographic studies have also revealed that one imine-phenoxy group with the *syn* C=N configuration functions as a bidentate ligand, whereas the other, of the *anti* C=N form, acts as a monodentate phenoxy ligand.

While Zr–IF catalysts **32** and **33** combined with MAO or *i*-Bu_3Al/$Ph_3CB(C_6F_5)_4$ exhibit low to moderate activity for ethylene polymerization, Ti–IF catalysts **30** and **31** on activa-
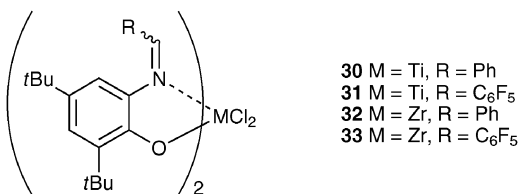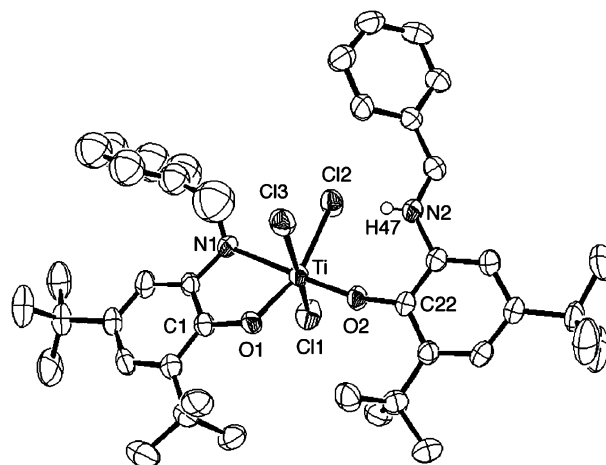

Fig. 23   Molecular structure of an IF catalyst **30**·HCl adduct (a zwitterionic complex).

tion with an appropriate activator convert ethylene to highly linear PEs with very high productivity (Table 9). When activated with MAO at 25 °C, Ti–IF catalyst **31** shows an extremely high activity of 19.9 kg-PE (mmol-cat h)$^{-1}$, which is comparable to those seen with Cp_2MCl_2/MAO (M = Ti; 16.7 kg-PE (mmol-cat h)$^{-1}$, M = Zr; 20.0 kg-PE (mmol-cat h)$^{-1}$). The very high activity obtained with Ti–IF catalyst **31**/MAO is probably ascribed to the effect of the electron-withdrawing C_6F_5 group on the imine-nitrogen. A similar effect of an electron-withdrawing substituent on the catalytic activity was observed for the II and FI catalysts.[38,62,73,74]

It should be emphasized that the Ti–IF catalyst **31** having a C_6F_5 group on the imine-nitrogen does not promote living ethylene polymerization, unlike the corresponding fluorinated Ti–FI catalysts capable of mediating highly controlled living

Table 8   Unique block copolymers created by fluorinated Ti–FI catalysts

	1st			2nd					3rd			
Entry	Segment	$10^{-3}M_n{}^a$	$M_n/M_n{}^a$	$T_m{}^b$/°C	Segment	$10^{-3}M_n{}^a$	$M_n/M_n{}^a$	P or H content^c	$T_m{}^b$/°C	Segment	$10^{-3}M_n{}^a$	$M_n/M_n{}^a$	P or H content^c	$T_m{}^b$/°C
1	PE	115	1.10	133	sPP	136	1.15	16.1	131	—	—	—	—	—
2	↑	↑	↑	↑	E/P^d	211	1.16	6.4	123	—	—	—	—	—
3	↑	↑	↑	↑	↑	↑	↑	↑	↑	sPP	235	1.15	14.1	123
4	↑	↑	↑	↑	↑	↑	↑	↑	↑	PE	272	1.14	6.6	120
5	sPP	27	1.13	137	E/P	161	1.51	40.3	127	—	—	—	—	—
6	PE	38	1.11	135	E/H^e	80	1.21	15.0	130	—	—	—	—	—

^{a} Determined by GPC. ^{b} Melting temperature measured by DSC. ^{c} Overall propylene (P) or 1-hexene (H) content (mol%): determined by ^{1}H NMR. ^{d} Poly(ethylene-*co*-propylene). ^{e} Poly(ethylene-*co*-1-hexene).

Table 9 Ethylene polymerization results with IF catalysts **30–33**

Entry	IF Catalyst/μmol	Co-catalyst[a]	$T/°C$	Activity[b]	$10^{-4}M_v$
1	**30** (5)	MAO	25	0.13	268
2	**30** (5)	Borate	25	0.07	—[c]
3	**30** (0.2)	Borate	75	21.4	64
4[e]	**30** (0.2)	Borate	75	18.7	59
5	**31** (0.2)	MAO	25	19.9	2.6
6	**31** (5)	Borate	25	0.16	171
7	**32** (5)	MAO	25	0.13	142
8	**32** (5)	Borate	25	0.18	—[c]
9	**33** (5)	MAO	25	0.04	—[d]
10	**33** (5)	Borate	25	0.08	—[c]

Conditions: atmospheric pressure, 5 min ([e]60 min), toluene 250 ml, ethylene gas feed 100 l h^{-1}. [a] MAO 1.25 mmol, borate (Ph$_3$CB(C$_6$F$_5$)$_4$ 6 μmol, *i*-Bu$_3$Al 50 μmol). [b] kg-PE (mmol-cat h)$^{-1}$. [c] Unavailable owing to low solubility of the polymer produced in decalin under the conditions for intrinsic viscosity measurement. [d] Unavailable due to low polymer yield.

Table 10 Ethylene polymerization results with FP catalysts **34** and **35**

Entry	FP catalyst	Co-catalyst	Activity[a]	$10^{-4}M_v$
1	**34**	MAO	0.037	417
2	**34**	Borate	0.227	323
3	**35**	MAO	0.009	368
4	**35**	Borate	0.006	200

Conditions: 25 °C, atmospheric pressure, 30 min, ethylene gas feed 100 l h^{-1}, complex 5.0 μmol, MAO (Al) 1.25 mmol, borate (Ph$_3$CB(C$_6$F$_5$)$_4$ 6 μmol, *i*-Bu$_3$Al 50 μmol), toluene 250 ml. [a] kg-polymer (mmol-cat h)$^{-1}$.

ethylene polymerization.[34–36] Interestingly, DFT calculation studies have demonstrated that there is virtually no interaction between the *ortho*-F and a β-H on the growing polymer chain (*ortho*-F/β-H distance 3.66 Å) for **31**/MAO catalyst system.[68]
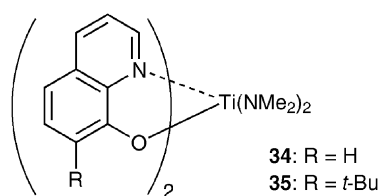
Conversely, Ti–IF catalyst **30** combined with *i*-Bu$_3$Al/Ph$_3$CB(C$_6$F$_5$)$_4$ displays enhanced activity as the temperature is increased (25–75 °C) and maintains very high activity for 60 min at 75 °C (18.7 kg-PE (mmol-cat h)$^{-1}$). ^{1}H NMR spectroscopic studies have suggested that a catalytically active species derived from Ti–IF catalyst **30** with *i*-Bu$_3$Al/Ph$_3$CB(C$_6$F$_5$)$_4$ is an amine-phenoxy ligated complex with a *i*-Bu$_2$Al group attached to the amine-donor, which is produced by the reduction of the imine functionality by *i*-Bu$_3$Al (and its contaminant *i*-Bu$_2$AlH). Similar reductions were observed for PI and FI catalysts.[59,75,76]

4.6 Phenoxy-pyridine ligated Ti complexes: FP catalysts

Inspired by the success of FI catalysts, we synthesized structurally related bis(phenoxy-pyridine) Ti complexes **34** and **35** (**34**: R = H, **35**: R = *t*-Bu), or FP catalysts, (the catalyst name "FP" is derived from the Japanese pronunciation of the ligand "*Fenokishi-Pirijin*") (Fig. 24), and evaluated their potential as ethylene polymerization catalysts.[69]
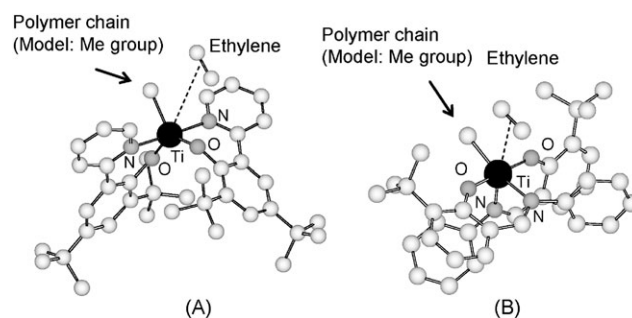
Although FP catalysts **34** and **35** provide active catalysts for the polymerization of ethylene after activation with MAO or *i*-Bu$_3$Al/Ph$_3$CB(C$_6$F$_5$)$_4$ at 25 °C, the catalysts exhibit only low to moderate catalytic activity independent of the substituent *ortho* to the phenoxy-oxygen (Table 10).

It should be pointed out that ethylene-coordinated cationic methyl complexes generated from FP catalysts **34** and **35** are suggested by DFT calculations to possess *cis*-located polymerization sites that are *trans* to the anionic donors (*i.e.*, phenoxy-

Fig. 25 Calculated structures of ethylene-coordinated cationic methyl species generated from FP catalyst **35** (A) and FI catalyst **24** (B).

oxygens) unlike the highly active catalysts such as PI catalysts,[59] II catalysts[38] and FI catalysts[75] described so far. Fig. 25 displays the DFT-optimized structures of catalytically active species stemming from FP catalyst **35** and FI catalyst **24** (for comparison).

As can be seen, a substituent *ortho* to the phenoxy-oxygen for FP catalyst **35** (Fig. 25(A)) is not effective for steric protection of the Ti center and for ion separation between the cationic active species and the anionic activator species as opposed to the substituent *ortho* to the phenoxy-oxygen for FI catalyst **24** (Fig. 25(B)), which explains the difference in polymerization behavior between FP and FI catalysts. Additionally, the presence of the anionic phenoxy-oxygens that are *trans* to the polymerization sites is presumably responsible for the lower activities exhibited by FP catalysts since the neutral imine-nitrogens *trans* to the polymerization sites play a crucial role in the achievement of high activity for FI catalysts, which is indicated by DFT calculations.[12,13,75]

5 Summary and outlook

The ligand oriented catalyst design concept has as its underlying basis the philosophy that electronically flexible properties of ligands are a necessary requirement for achieving high activity. This concept has resulted in the discovery of a number of new olefin polymerization catalysts represented by PI, II, FI and IF catalysts, that show exceptional activity for ethylene polymerization.

These new catalysts have created a variety of new value-added polymers, such as selective vinyl- and Al-terminated

Fig. 24 Structures of FP catalysts **34** and **35**.

34: R = H
35: R = *t*-Bu

PEs, ultra-high-molecular-weight (co)polymers, high-tacticity PPs, regio- and stereoirregular high-molecular-weight poly-(higher α-olefin)s and various block copolymers from ethylene, propylene, higher α-olefins and norbornene, many of which were previously unobtainable using conventional catalysts.

Research on these catalysts has yielded useful information on high catalytic activity, the formation of highly syndiotactic PPs with C_2-symmetric catalysts, the origin of highly controlled living olefin polymerization, and the high-incorporation ability of higher α-olefins and norbornene.

All of which means that ligand-oriented catalyst design concept based catalysts have made a significant impact on polymer synthesis and polymerization catalysis. Olefin polymerization will continue to grow in importance as a field central to catalysis science and polymer science in general. I sincerely believe that further research based on the ligand oriented catalyst design concept will continue to uncover high-activity catalysts capable of producing unique polymer structures. These advances will greatly expand the range of olefin-based polymers and will provide further insight into polymerization catalysis.

Acknowledgements

References

1 H. H. Brintzinger, D. Fisher, R. Mülhaupt, B. Rieger and R. M. Waymouth, *Angew. Chem., Int. Ed. Engl.*, 1995, **34**, 1143.
2 M. Bochmann, *J. Chem. Soc., Dalton Trans.*, 1996, 255.
3 A. L. McKnight and R. M. Waymouth, *Chem. Rev.*, 1998, **98**, 2587.
4 G. J. P. Britovsek, V. C. Gibson and D. F. Wass, *Angew. Chem., Int. Ed.*, 1999, **38**, 428.
5 S. D. Ittel, L. K. Johnson and M. Brookhart, *Chem. Rev.*, 2000, **100**, 1169.
6 V. C. Gibson and S. K. Spitzmesser, *Chem. Rev.*, 2003, **103**, 283.
7 Y. Suzuki, H. Terao and T. Fujita, *Bull. Chem. Soc. Jpn.*, 2003, **76**, 1493.
8 D. W. Stephan, *Organometallics*, 2005, **24**, 2548.
9 P. D. Bolton and P. Mountford, *Adv. Synth. Catal.*, 2005, **347**, 355.
10 V. C. Gibson, C. Redshaw and G. A. Solan, *Chem. Rev.*, 2007, **107**, 1745.
11 S. Matsui and T. Fujita, *Catal. Today*, 2001, **66**, 63.
12 H. Makio, N. Kashiwa and T. Fujita, *Adv. Synth. Catal.*, 2002, **344**, 477.
13 M. Mitani, J. Saito, S. Ishii, Y. Nakayama, H. Makio, N. Matsukawa, S. Matsui, J. Mohri, R. Furuyama, H. Terao, H. Bando, H. Tanaka and T. Fujita, *Chem. Rec.*, 2004, **4**, 137.
14 Y. Yoshida, S. Matsui and T. Fujita, *J. Organomet. Chem.*, 2005, **690**, 4382.
15 N. Nakayama, J. Saito, H. Bando and T. Fujita, *Chem.–Eur. J.*, 2006, **12**, 7546.
16 K. Kawai, T. Kitahara and T. Fujita, *Jpn. Pat.*, 1996, 325283.
17 K. Kawai, T. Kitahara and T. Fujita, *Jpn. Pat.*, 1996, 325315.
18 Y. Suzuki, T. Oshiki, H. Tanaka, K. Takai and T. Fujita, *Chem. Lett.*, 2005, **34**, 1458.
19 S. Ishii, M. Mitani, J. Saito, S. Matsuura, S. Kojoh, N. Kashiwa and T. Fujita, *Chem. Lett.*, 2002, 740.
20 H. Terao, S. Ishii, J. Saito, S. Matsuura, M. Mitani, N. Nagai, H. Tanaka and T. Fujita, *Macromolecules*, 2006, **39**, 8584.
21 J. Saito, Y. Tohi, N. Matsukawa, M. Mitani and T. Fujita, *Macromolecules*, 2005, **38**, 4955.
22 Y. Tohi, H. Makio, S. Matsui, M. Onda and T. Fujita, *Macromolecules*, 2003, **36**, 523.
23 Y. Tohi, T. Nakano, H. Makio, S. Matsui, T. Fujita and T. Yamaguchi, *Macromol. Chem. Phys.*, 2004, **205**, 1179.
24 S. Ishii, J. Saito, S. Matsuura, Y. Suzuki, R. Furuyama, M. Mitani, T. Nakano, N. Kashiwa and T. Fujita, *Macromol. Rapid Commun.*, 2002, **23**, 693.
25 J. Saito, M. Mitani, S. Matsui, N. Kashiwa and T. Fujita, *Macromol. Rapid Commun.*, 2000, **21**, 1333.
26 J. Saito, Y. Suzuki and T. Fujita, *Chem. Lett.*, 2003, **32**, 236.
27 J. Saito, Y. Suzuki, H. Makio, H. Tanaka, M. Onda and T. Fujita, *Macromolecules*, 2006, **39**, 4023.
28 J. Saito, M. Onda, S. Matsui, M. Mitani, R. Furuyama, H. Tanaka and T. Fujita, *Macromol. Rapid Commun.*, 2002, **23**, 1118.
29 A. V. Prasad, H. Makio, J. Saito, M. Onda and T. Fujita, *Chem. Lett.*, 2004, **33**, 250.
30 R. Furuyama, J. Saito, S. Ishii, M. Mitani, S. Matsui, Y. Tohi, H. Makio, N. Matsukawa, H. Tanaka and T. Fujita, *J. Mol. Catal. A: Chem.*, 2003, **200**, 31.
31 J. Tian and G. W. Coates, *Angew. Chem., Int. Ed.*, 2000, **39**, 3626.
32 H. Makio and T. Fujita, *Bull. Chem. Soc. Jpn.*, 2005, **78**, 52.
33 For the first report on syndiospecific propylene polymerization, living ethylene and propylene polymerization, and block copolymer synthesis with Ti–FI catalysts, see: M. Mitani, Y. Yoshida, J. Mohri, K. Tsuru, S. Ishii, S. Kojoh, T. Matsugi, J. Saito, N. Matsukawa, S. Matsui, T. Nakano, H. Tanaka, N. Kashiwa and T. Fujita, *WO Pat.*, 01/55231 (filed in January 2000).
34 Mitani, T. Nakano and T. Fujita, *Chem.–Eur. J.*, 2003, **9**, 2396.
35 R. Furuyama, J. Saito, S. Ishii, H. Makio, M. Mitani, H. Tanaka and T. Fujita, *J. Organomet. Chem.*, 2005, **690**, 4398.
36 A. Sakuma, M.-S. Weiser and T. Fujita, *Polym. J.*, 2007, **39**, 193.
37 G. J. Domski, J. M. Rose, G. W. Coates, A. D. Bolig and M. Brookhart, *Prog. Polym. Sci.*, 2007, **32**, 30.
38 T. Matsugi, S. Matsui, S. Kojoh, Y. Takagi, Y. Inoue, T. Nakano, T. Fujita and N. Kashiwa, *Macromolecules*, 2002, **35**, 4880.
39 Y. Yoshida, J. Mohri, S. Ishii, M. Mitani, J. Saito, S. Matsui, H. Makio, T. Nakano, H. Tanaka, M. Onda, Y. Yamamoto, A. Mizuno and T. Fujita, *J. Am. Chem. Soc.*, 2004, **126**, 12023.
40 D. A. Pennington, S. J. Coles, M. B. Hursthouse, M. Bochmann and S. J. Lancaster, *Chem. Commun.*, 2005, 3150.
41 D. M. Dawson, D. A. Walker, M. T. Pett and M. Bochmann, *J. Chem. Soc., Dalton Trans.*, 2000, 459.
42 G. Talarico, V. Busico and L. Cavallo, *J. Am. Chem. Soc.*, 2003, **125**, 7172.
43 J. Huang, B. Lian, Y. Qian, W. Zhou, W. Chen and G. Zheng, *Macromolecules*, 2002, **35**, 4871.
44 J. R. Severn and J. C. Chadwick, *Macromol. Rapid Commun.*, 2004, **25**, 1024.
45 R. A. E. Cherian, E. B. Lobkovsky and G. W. Coates, *Macromolecules*, 2005, **38**, 6259.
46 J. Strauch, T. H. Warren, G. Erker, R. Fröhlich and P. Saarenketo, *Inorg. Chim. Acta*, 2000, **300–302**, 810.
47 V. C. Gibson, P. J. Maddox, C. Newton, C. Redshaw, G. A. Solan, A. J. P. White and D. J. Williams, *Chem. Commun.*, 1998, 1651.
48 M. Van Meurs, G. J. P. Britovsek, V. C. Gibson and S. A. Cohen, *J. Am. Chem. Soc.*, 2005, **127**, 9913.
49 A. L. Johnson, M. G. Davidson, M. D. Lunn and M. F. Mahon, *Eur. J. Inorg. Chem.*, 2006, **15**, 3088.
50 K. Mashima and H. Tsurugi, *J. Organomet. Chem.*, 2005, **690**, 4414.
51 M.-S. Weiser and R. Mülhaupt, *Macromol. Rapid Commun.*, 2006, **27**, 1009.
52 M. Lamberti, M. Consolmagno, M. Mazzeo and C. Pellecchia, *Macromol. Rapid Commun.*, 2005, **26**, 1866.
53 A. Parssinen, T. Luhtanen, M. Klinga, T. Pakkanen, M. Leskela and T. Repo, *Organometallics*, 2007, **26**, 3690.
54 R. K. J. Bott, M. Hammond, P. N. Horton, S. J. Lancaster, M. Bochmann and P. Scott, *Dalton Trans.*, 2005, 3611.

55 K. P. Bryliakov, E. A. Kravtsov, D. A. Pennington, S. J. Lancaster, M. Bochmann, H. H. Brintzinger and E. P. Talsi, *Organometallics*, 2005, **24**, 5660.

56 K. Vanka, Z. Xu and T. Ziegler, *Organometallics*, 2004, **23** 2900.

57 D. J. Arriola, E. M. Carnahan, P. D. Hustad, R. L. Kuhlman and T. T. Wenzel, *Science*, 2006, **312**, 714.

58 Y. Yoshida, S. Matsui, Y. Takagi, M. Mitani, M. Nitabaru, T. Nakano, H. Tanaka and T. Fujita, *Chem. Lett.*, 2000, 1270.

59 Y. Yoshida, S. Matsui, Y. Takagi, M. Mitani, T. Nakano, H. Tanaka, N. Kashiwa and T. Fujita, *Organometallics*, 2001, **20**, 4793.

60 Y. Yoshida, J. Saito, M. Mitani, Y. Takagi, S. Matsui, S. Ishii, T. Nakano, N. Kashiwa and T. Fujita, *Chem. Commun.*, 2002, 1298.

61 Y. Yoshida, T. Nakano, H. Tanaka and T. Fujita, *Isr. J. Chem.*, 2002, **42**, 353.

62 T. Matsugi, S. Matsui, S. Kojoh, Y. Takagi, Y. Inoue, T. Fujita and N. Kashiwa, *Chem. Lett.*, 2001, 566.

63 Y. Suzuki, Y. Inoue, H. Tanaka and T. Fujita, *Macromol. Rapid Commun.*, 2004, **25**, 493.

64 S. Matsui, Y. Tohi, M. Mitani, J. Saito, H. Makio, H. Tanaka, M. Nitabaru, T. Nakano and T. Fujita, *Chem. Lett.*, 1999, 1065.

65 S. Matsui, M. Mitani, J. Saito, Y. Tohi, H. Makio, H. Tanaka and T. Fujita, *Chem. Lett.*, 1999, 1263.

66 S. Matsui, M. Mitani, J. Saito, N. Matsukawa, H. Tanaka, T. Nakano and T. Fujita, *Chem. Lett.*, 2000, 554.

67 Y. Suzuki, N. Kashiwa and T. Fujita, *Chem. Lett.*, 2002, 358.

68 Y. Suzuki, H. Tanaka, T. Oshiki, K. Takai and T. Fujita, *Chem.–Asian J.*, 2006, **1**, 878.

69 Y. Inoue, T. Nakano, H. Tanaka, N. Kashiwa and T. Fujita, *Chem. Lett.*, 2001, 1060.

70 S. Matsui, T. P. Spaniol, Y. Takagi, Y. Yoshida and J. Okuda, *J. Chem. Soc., Dalton Trans.*, 2002, 4017.

71 S. Matsui, Y. Yoshida, Y. Takagi, T. P. Spaniol and J. Okuda, *J. Organomet. Chem.*, 2004, **689**, 1155.

72 N. Matsukawa, S. Matsui, M. Mitani, J. Saito, K. Tsuru, N. Kashiwa and T. Fujita, *J. Mol. Catal. A: Chem.*, 2001, **169**, 99.

73 S. Ishii, J. Saito, M. Mitani, J. Mohri, N. Matsukawa, Y. Tohi, S. Matsui, N. Kashiwa and T. Fujita, *J. Mol. Catal. A: Chem.*, 2002, **179**, 11.

74 S. Ishii, R. Furuyama, N. Matsukawa, J. Saito, M. Mitani, H. Tanaka and T. Fujita, *Macromol. Rapid Commun.*, 2003, **24**, 452.

75 S. Matsui, M. Mitani, J. Saito, Y. Tohi, H. Makio, N. Matsukawa, Y. Takagi, K. Tsuru, M. Nitabaru, T. Nakano, H. Tanaka, N. Kashiwa and T. Fujita, *J. Am. Chem. Soc.*, 2001, **123**, 6847.

76 J. Saito, M. Mitani, S. Matsui, Y. Tohi, H. Makio, T. Nakano, H. Tanaka, N. Kashiwa and T. Fujita, *Macromol. Chem. Phys.*, 2002, **203**, 59.

77 Y. Nakayama, H. Bando, Y. Sonobe, H. Kaneko, N. Kashiwa and T. Fujita, *J. Catal.*, 2003, **215**, 171.

78 Y. Nakayama, H. Bando, Y. Sonobe and T. Fujita, *J. Mol. Catal. A: Chem.*, 2004, **213**, 141.

79 Y. Nakayama, H. Bando, Y. Sonobe and T. Fujita, *Bull. Chem. Soc. Jpn.*, 2004, **77**, 617.

80 H. Makio and T. Fujita, *Macromol. Rapid Commun.*, 2007, **28**, 698.

81 H. Makio, Y. Tohi, J. Saito, M. Onda and T. Fujita, *Macromol. Rapid Commun.*, 2003, **24**, 894.

82 J. Saito, M. Mitani, Y. Yoshida, S. Matsui, J. Mohri, S. Ishii, S. Kojoh, N. Kashiwa and T. Fujita, *Angew. Chem., Int. Ed.*, 2001, **40**, 2918.

83 J. Saito, M. Mitani, J. Mohri, S. Ishii, Y. Yoshida, T. Matsugi, S. Kojoh, N. Kashiwa and T. Fujita, *Chem. Lett.*, 2001, 576.

84 J. Tian, P. D. Hustad and G. W. Coates, *J. Am. Chem. Soc.*, 2001, **123**, 5134.

85 M. Mitani, J. Mohri, Y. Yoshida, J. Saito, S. Ishii, K. Tsuru, S. Matsui, R. Furuyama, T. Nakano, H. Tanaka, S. Kojoh, T. Matsugi, N. Kashiwa and T. Fujita, *J. Am. Chem. Soc.*, 2002, **124**, 3327.

86 M. Mitani, R. Furuyama, J. Mohri, J. Saito, S. Ishii, H. Terao, N. Kashiwa and T. Fujita, *J. Am. Chem. Soc.*, 2002, **124**, 7888.

87 M. Mitani, R. Furuyama, J. Mohri, J. Saito, S. Ishii, H. Terao, T. Nakano, H. Tanaka and T. Fujita, *J. Am. Chem. Soc.*, 2003, **125**, 4293.

88 G. Milano, L. Cavallo and G. Guerra, *J. Am. Chem. Soc.*, 2002, **124**, 13368.

89 J. Saito, M. Mitani, M. Onda, J. Mohri, S. Ishii, Y. Yoshida, T. Nakano, H. Tanaka, T. Matsugi, S. Kojoh, N. Kashiwa and T. Fujita, *Macromol. Rapid Commun.*, 2001, **22**, 1072.

90 M. Lamberti, D. Pappalardo, A. Zambelli and C. Pellecchia, *Macromolecules*, 2002, **35**, 658.

91 P. D. Hustad, J. Tian and G. W. Coates, *J. Am. Chem. Soc.*, 2002, **124**, 3614.

92 H. Makio, T. Oshiki, K. Takai and T. Fujita, *Chem. Lett.*, 2005, **34**, 1382.

93 H. Makio and T. Fujita, *Macromol. Symp.*, 2004, **213**, 221.

94 G. Talarico, V. Busico and L. Cavallo, *Organometallics*, 2004, **23**, 5989.

95 S. Kojoh, T. Matsugi, J. Saito, M. Mitani, T. Fujita and N. Kashiwa, *Chem. Lett.*, 2001, 822.

96 R. Furuyama, M. Mitani, J. Mohri, R. Mori, H. Tanaka and T. Fujita, *Macromolecules*, 2005, **38**, 1546.

97 M. Mitani, J. Mohri, R. Furuyama, S. Ishii and T. Fujita, *Chem. Lett.*, 2003, **32**, 238.

98 S. S. Ono, T. Matsugi, O. Matsuoka, S. Kojoh, T. Fujita, N. Kashiwa and S. Yamamoto, *Chem. Lett.*, 2003, **32**, 1182.

This journal is © The Royal Society of Chemistry 2008

Chem. Soc. Rev., 2008, **37**, 1264–1277 | 1277